REVISTA INTERDISCIPLINAR DE PESQUISA EM ENGENHARIA

CILAMCE 2016

XXXVII IBERIAN LATIN AMERICAN CONGRESS ON COMPUTATIONAL METHODS IN ENGINEERING
BRASÍLIA - DF - BRAZIL

GFEM NONLINEAR ANALYSIS USING AN ELASTOPLASTIC DAMAGE CONSTITUTIVE MODEL

Anelize Borges Monteiro

ane.lize.eng@gmail.com

Anderson Renato Vobornik Wolenski

andersonwolenski@gmail.com

Felício Bruzzi Barros

feliciobbarros@gmail.com

Roque Luiz da Silva Pitangueira

roquepitangueira@gmail.com

Samuel Silva Penna

spenna@dees.ufmg.br

Universidade Federal de Minas Gerais. Av. Antonio Carlos, 6627, Belo Horizonte, MG, Brazil

Abstract. *The Generalized Finite Element Method (GFEM) has been developed with the purpose of overcoming some limitations inherent to the Finite Element Method (FEM), related to problems that require remeshing. FEM solution space is enriched with a priori known information through the Partition of Unity (PU) at GFEM. Certain obstacles related to the nonlinear analysis can be mitigated with the use of GFEM and the damage and plasticity fronts can be represented. A FEM computational environment has been previously expanded with the enclosing of the GFEM formulation to linear analysis with minimum impact in the code structure and with requirements for extensibility and robustness. Such environment, so-called INSANE (INteractive Structural ANalysis Environment), is an object-oriented system that allows linear and nonlinear, static and dynamic structural analysis. Numerical simulations applying an elastoplastic damage constitutive model are carried out aiming to demonstrate the versatility of the code related to the application of such a constitutive model and GFEM.*

Keywords: *Nonlinear Analysis, GFEM, Elastoplastic Damage Constitutive Model.*

1 INTRODUCTION

Several engineering problems use partial differential equations relating field variables inside a particular domain. To obtain the analytical solution it is used some numerical method since such problems have complex geometry and boundary conditions. In this context, it was developed the Finite Element Method (FEM), which is an efficient numerical resource to solve boundary value problems. Additionally, nowadays it is impossible to project innovative structures without FEM and the use of computational programs based on this method became easier due to the development of pre-processor and post-processor tools that provide interactive graphics resources.

Nonetheless, there are phenomena whose behavior can not be satisfactorily described by conventional FEM and this fact has motivated the development of new strategies. Problems subjected to large deformations and to crack and damage propagation require modifications in discretization of the structure (remeshing) and methods such as Generalized Finite Element Method (GFEM) have been developed to solve these and others issues.

The Generalized Finite Element Method (Melenk and Babuška (1996); Duarte *et al.* (2000)) can be considered as originated from the so-called meshless methods proposed in the 1990s. In spite of its theoretical bases be well established, there is an extensive area of research and of numerical experimentation to be investigated. According to Barros (2002), GFEM is formulated in a way that the numerical simulation guarantees certain independence of the mesh of finite elements. The relative mesh independence can be observed by the possibility of introducing special functions on numerical approximation, without modifying the mesh, and by the relative insensitivity to angular distortion of the elements.

Concerning Constitutive Modeling, one of the most used frameworks is the Plasticity Theory. According to this theory, the inelastic behavior of the materials is described by the quantification of plastic strain increase. Lemaitre (1984) has verified by means of experimental tests in many materials that the energy dissipation associated with nucleation and growth of voids and microcracks, which accompanies the growth of plastic strain, had a dominant effect.

In this context, this paper presents an Elastoplastic Damage Constitutive Model proposed by Lemaitre (1985a,1985b), with the possibility of adoption of different hardening/softening laws to description of the material's inelastic behavior. The computational implementation of this model was done on the `INSANE` system according to Monteiro *et al.* (2013).

`INSANE` is a computational environment developed at the Department of Structural Engineering of the Federal University of Minas Gerais (UFMG). This system is implemented in Java language and uses the paradigm of Object Oriented Programming. The platform was designed with the purpose of being a segmented system, friendly and capable to support new implementations without significant modifications. In addition, its library is composed of many modules which allow developers to perform simultaneous and independent implementations.

2 THERMODYNAMICS OF IRREVERSIBLE PROCESSES

According to Coleman and Gurtin (1967), together with heat conduction, dissipative effects follow strains and they can be considered of different ways. Among the main forms, the authors have highlighted the one which postulates the existence of internal state variables that influence the free energy and whose variation rates are governed by differential equations.

2.1 Potential State

Thermodynamic state of a system can be completely determined by a finite number of state variables, related to the phenomena that the model will describe. These variables are divided into two categories: observable and internal. Observable variables can be measured experimentally and internal variables are not directly quantified and they are related to dissipative mechanisms.

Murakami (2012) asserts that the adoption of the observable variables *total strain* $\boldsymbol{\varepsilon}$ and *temperature* T allows elucidating a number of mechanical phenomena, such as elastic, viscoelastic and plastic deformations as well as damage and fracture. The author declares that the internal variables, on the other hand, must be selected so that they can represent adequately the change of internal state of the material. Thus the selection of the internal variables depends on the phenomena to be described.

Defined the observable variables ($\boldsymbol{\varepsilon}$ and T) and the internal variables R and D, where, by assuming the isotropy of damage, the damage state can be described by a scalar damage variable D and the scalar variable R is referred to as the isotropic hardening or softening variable, it is postulated the existence of a thermodynamic potential of which the state laws can be derived. The potential state is written as a function of the state variables. Assuming that the deformation and displacement are small, the *Helmholtz free energy* is a possible potential:

$$\psi = \psi(\boldsymbol{\varepsilon},\ T,\ R,\ D). \tag{1}$$

It is assumed that the total strain, $\boldsymbol{\varepsilon}$, may be divided into the sum of the elastic and plastic strains:

$$\boldsymbol{\varepsilon} = \boldsymbol{\varepsilon}^e + \boldsymbol{\varepsilon}^p. \tag{2}$$

Since the effect of $\boldsymbol{\varepsilon}^p$ may be expressed in terms of the internal variable, the free energy can be written as a function of the elastic strain, temperature and internal variables:

$$\psi = \psi(\boldsymbol{\varepsilon}^e,\ T,\ R,\ D). \tag{3}$$

Therefore, the rate of change of this energy is given by:

$$\dot{\psi} = \frac{\partial \psi}{\partial \boldsymbol{\varepsilon}^e} : \dot{\boldsymbol{\varepsilon}}^e + \frac{\partial \psi}{\partial T}\dot{T} + \frac{\partial \psi}{\partial R}\dot{R} + \frac{\partial \psi}{\partial D}\dot{D}. \tag{4}$$

In the thermodynamics of irreversible processes, a system is in thermodynamic equilibrium if, for certain state, the values of the state variables are independent of time. In this context, conservation of energy of a system is treated by the first law of thermodynamics, while the second law imposes that in any process of transformation of a system, the total entropy variation must be equal or overcome the variation caused by the heat transfer.

First and second laws may be combined, leading to an inequality that must be observed in order to a process is thermodynamically admissible. The *Clausius-Duhem inequality* must be satisfied for every thermodynamic process of the continuum, according to Malvern (1969). Thus, this inequality imposes essential restrictions on constitutive equations and ensures the

thermodynamic foundation of the constitutive theory for the dissipative processes of a continuum. This inequality is defined by:

$$\boldsymbol{\sigma} : \dot{\boldsymbol{\varepsilon}} - \rho(\dot{\psi} + \dot{T}\mathrm{s}) - \mathbf{q}.\frac{grad\, T}{T} \geq 0, \tag{5}$$

where ρ is the mass density, $\mathbf{q}$ is the heat flux vector and s is the entropy density.

Substituting (2) and (4) on the Clausius-Duhem inequality, it is obtained:

$$\begin{aligned}\left(\boldsymbol{\sigma} - \rho\frac{\partial\psi}{\partial\boldsymbol{\varepsilon}^e}\right) : \dot{\boldsymbol{\varepsilon}}^e - \rho\left(s + \frac{\partial\psi}{\partial T}\right)\dot{T} \quad &+ \quad \boldsymbol{\sigma} : \dot{\boldsymbol{\varepsilon}}^p - \rho\frac{\partial\psi}{\partial R}\dot{R} \\ &- \quad \rho\frac{\partial\psi}{\partial D}\dot{D} - \frac{grad\, T}{T}\mathbf{q} \geq 0.\end{aligned} \tag{6}$$

This expression must satisfy all thermodynamic processes described by the equation (3). Therefore, supposing that the medium is subject only to elastic strain and uniform temperature and that the internal variables remains unchanged, it is written:

$$grad\, T = 0;\;\; \dot{\boldsymbol{\varepsilon}}^p = 0;\;\; \dot{R} = 0;\;\; \dot{D} = 0. \tag{7}$$

Thus, inequality (6) is rewritten as:

$$\left(\boldsymbol{\sigma} - \rho\frac{\partial\psi}{\partial\boldsymbol{\varepsilon}^e}\right) : \dot{\boldsymbol{\varepsilon}}^e - \rho\left(\mathrm{s} + \frac{\partial\psi}{\partial T}\right)\dot{T} \geq 0. \tag{8}$$

This inequality should be satisfied for any choice of $\dot{\boldsymbol{\varepsilon}}^e$ and $\dot{T}$, and hence it is presented the definition to stress associated to the state variable $\boldsymbol{\varepsilon}^e$:

$$\boldsymbol{\sigma} = \rho\frac{\partial\psi}{\partial\boldsymbol{\varepsilon}^e}, \tag{9}$$

and to the entropy associated to the state variable T:

$$\mathrm{s} = -\frac{\partial\psi}{\partial T}. \tag{10}$$

In this way, the potential state, provided by the Helmholtz free energy, defines the state laws given by the equations (9) and (10), which allow writing the relations between the observable state variables and the variables associated with them, being the constitutive equations of the material medium.

2.2 Dissipation Potential

From the previous section, it is possible to observe that the potential state allows writing the relations between the observable and associated variables. According to Lemaitre and Chaboche (1990), to the internal variables, the potential state is able to define their associated variables, but not to establish relations between them. Thus, the description of the dissipation process, related to the internal variables evolution, needs evolution equations (or complementary equations), determined by a dissipation potential.

The dissipation potential is a scalar function written in terms of associated variables whose objective is establishing evolution laws to the internal variables.

The substitution of equations (9) and (10) on inequation (6) leads to:

$$\boldsymbol{\sigma} : \dot{\boldsymbol{\varepsilon}}^p - \rho\frac{\partial\psi}{\partial R}\dot{R} - \rho\frac{\partial\psi}{\partial D}\dot{D} - \frac{grad\, T}{T}.\mathbf{q} \geq 0. \tag{11}$$

In a state where the temperature is uniform ($grad\, T = 0$), the associated variables may be defined as:

$$\kappa \equiv \rho\frac{\partial\psi}{\partial R}, \tag{12}$$

where κ is the associated variable with the internal variable R and

$$Y \equiv -\rho\frac{\partial\psi}{\partial D}, \tag{13}$$

where Y is the associated variable with the internal variable D.

It is possible to write:

$$\mathbf{d} = \boldsymbol{\sigma} : \dot{\boldsymbol{\varepsilon}}^p - \kappa\dot{R} + Y\dot{D} \geq 0. \tag{14}$$

For the dissipation process of inequation (14), the generalized flux vector $\mathbf{J}$ and the generalized force vector $\mathbf{X}$ are defined by:

$$\mathbf{J} \equiv \{\dot{\boldsymbol{\varepsilon}}^p,\ \dot{R},\ \dot{D}\}; \tag{15}$$

$$\mathbf{X} \equiv \{\boldsymbol{\sigma},\ -\kappa,\ -Y\}. \tag{16}$$

Then, inequation (14) is expressed in a compact form:

$$\mathbf{d} = \mathbf{X} \cdot \mathbf{J} \geq 0. \tag{17}$$

When the dissipation $\mathbf{d}$ is expressed in the form of inequation (14), the evolution equation for the generalized flux vector $\mathbf{J}$ can be derived from a potential function Q of the generalized force $\mathbf{X}$. Then, it is postulated a dissipation potential function in the form:

$$Q(\mathbf{X}) = Q(\boldsymbol{\sigma},\ \kappa,\ -Y;\ \boldsymbol{\varepsilon}^p,\ R,\ D). \tag{18}$$

This dissipation potential function may be divided into two parts: the dissipation potential due to the plastic deformation, Q^p, and the dissipation potential due to the damage, Q^d:

$$Q(\boldsymbol{\sigma},\ \kappa, -Y) = Q^p(\boldsymbol{\sigma},\ \kappa,\ D) + Q^d(-Y,\ D). \tag{19}$$

The plastic dissipation potential Q^p plays the role of *yield surface* in the space of the generalized forces:

$$Q^p(\boldsymbol{\sigma},\ \kappa,\ D) = 0. \tag{20}$$

This potential defines the plasticization criterion and the occurrence of dissipative phenomena and it is a function that allows evaluating loading and unloading conditions of the model. Based on the *von Mises yielding criterion*, it is define the following yield surface:

$$Q^p = \frac{\sqrt{3J_2(\mathbf{s})}}{1-D} - \sigma_0 - \kappa, \tag{21}$$

where σ_0 is the uniaxial yield stress of the undamaged material and $J_2(\mathbf{s})$ is the second stress deviator invariant, written as:

$$J_2(\mathbf{s}) = \frac{1}{2} s_{ij} s_{ij}, \tag{22}$$

where the stress deviator is defined by:

$$s_{ij} = \sigma_{ij} - \frac{1}{3}\sigma_{ij}\delta_{ij}, \tag{23}$$

where δ_{ij} is the *Krönecker delta*.

Lemaitre (1985b) defined Q^d as a function of the damage energy release rate Y:

$$Q^d = \frac{r}{(1-D)(S+1)} \left(\frac{-Y}{r}\right)^{S+1}, \tag{24}$$

where r and S are material constants. According to Lemaitre *et al.* (1999), r is denominated *damage strength* and quantifies the damage per strain increment and S is the *damage exponent* that represents the nonlinearity of the damage process.

The evolution of the dissipative variables that compose the vector $\mathbf{J}$ may be calculated through the function Q as:

$$\mathbf{J} = \dot{\gamma} \frac{\partial Q}{\partial \mathbf{X}}, \tag{25}$$

where $\dot{\gamma}$ is the indeterminate multiplier of plastic and damage evolution equation. Therefore, it is possible to explicit the dissipative variables rates:

$$\dot{\varepsilon}^p_{ij} = \dot{\gamma} \frac{\partial Q^p}{\partial \sigma_{ij}} = \sqrt{\frac{3}{2}} \frac{s_{ij}}{(1-D)\|s_{ij}\|}; \tag{26}$$

$$\dot{R} = -\dot{\gamma} \frac{\partial Q^p}{\partial \kappa} = \dot{\gamma}; \tag{27}$$

$$\dot{D} = \dot{\gamma} \frac{\partial Q^d}{\partial (-Y)} = \dot{\gamma} \frac{1}{1-D} \left(\frac{-Y}{r}\right)^S, \tag{28}$$

where equation (26) represents the plastic strain evolution, equation (27) defines the evolution of the hardening or softening variable and equation (28) represents the damage evolution.

3 INCLUSION OF THE ELASTOPLASTIC DAMAGE MODEL ON THE UNIFIED ENVIRONMENT

Penna (2011) reported that many strands of the constitutive modeling are based on theoretical frameworks capable of representing the main characteristics of the material medium, capturing the experimentally observed behaviors and providing a more realistic model. The author emphasized which, after the development of a large number of elastoplastic and elastic degradation constitutive models, attempts of unification to represent, in the same theoretical structure, various descriptions of the material behavior were observed. In this context, Penna (2011) presented an expansion of the theoretical framework proposed by Carol *et al.* (1994), capable to contemplate various constitutive models (elastoplastic or elastic degradation; isotropic, orthotropic or anisotropic), formulated with a single or multiple potential functions and based on strain, stress, thermodynamic forces or damage variables. Such theoretical framework is based on common hypothesis to elastoplastic and elastic degradation models to describe the material medium.

Initially, it is established a relation between stress and strain:

$$\sigma_{ij} = E_{ijkl}\varepsilon_{kl} \ , \tag{29}$$

where σ_{ij} are the stress tensor components, E_{ijkl} are the stiffness tensor components and ε_{kl} are the strain tensor components.

Then, one or more potential functions are defined:

$$F_n = F_n(\boldsymbol{\sigma}, \mathbf{p}), \tag{30}$$

where $n = 1, 2, ..., n$ represents de number of potential functions, $\boldsymbol{\sigma}$ is the stress tensor and $\mathbf{p}$ is a vector that contains the internal variables.

The tangent operator is defined by:

$$E^t_{ijkl} = E_{ijkl} + \frac{1}{\bar{H}_{nm}}\bar{n}_{nij}\bar{m}_{mkl} \ , \tag{31}$$

where the tensors $\bar{\mathbf{n}}$, $\bar{H}$ and $\bar{\mathbf{m}}$ must be determined. For notation, when the formulation is based on strain the tensors are represented with a bar. Otherwise, the formulation is based on stress.

Penna (2011) highlighted the formulations based on stress and strain are said dual. According to the author, the potential functions written in terms of stress or strain provide mathematical expressions with different terms, but for the same state of stress or the corresponding strain state, they generate the same result. Thus, it is possible to relate the tensor components of the gradients of the formulations based on stress and strain. Therefore, a model based on stress may be written in terms of strain and vice versa.

The dissipation potential function defined by Lemaitre (1985a,1985b) is given by:

$$Q(\sigma_{ij},\ \kappa,\ D,\ -Y) = \frac{\sqrt{3J_2(\mathbf{s})}}{1-D} - \sigma(\kappa) + \frac{r}{(1-D)(S+1)}\left(\frac{-Y}{r}\right)^{S+1} . \tag{32}$$

n_{kl} are the evolution directions of the yield surface tensor components in the stress domain, defined by:

$$n_{kl} = \left.\frac{\partial Q^p}{\partial \sigma_{kl}}\right|_{p=constant} = \sqrt{\frac{3}{2}}\frac{s_{kl}}{(1-D)\|s_{kl}\|}. \tag{33}$$

Since the model proposed by Lemaitre (1985a,1985b) has one potential function (Q) and one variable related to the hardening or softening (κ), the hardening-softening modulus tensor components H_{nm} are written as:

$$H_{nm} = -\frac{\partial Q^p}{\partial R}\bigg|_{\boldsymbol{\sigma}=constant} = -\frac{\partial Q^p}{\partial \sigma(\kappa)}\frac{\partial \sigma(\kappa)}{\partial R} = -(-1)\mathscr{H} = \mathscr{H}. \tag{34}$$

The dissipative processes evolution is define from the tensor $\mathbf{m}$:

$$m_{kl} = \frac{\partial Q^d}{\partial \sigma_{kl}}\bigg|_{p=constant}. \tag{35}$$

When do not exist an explicit function to the dissipation potential in terms, in this case, of σ_{kl}, it is possible to redefine $\mathbf{m}$ as:

$$m_{ij} = M_{ijkl}\sigma_{kl}\ , \tag{36}$$

where M_{ijkl} defines the direction of the rate of change of the compliance tensor and it is obtained through the Degradation Rule as:

$$M_{ijkl} = \frac{\partial C_{ijkl}}{\partial D}\mathscr{M}\ , \tag{37}$$

where D is the scalar damage variable, $\mathscr{M}$ is the variable that denotes the direction of the rate of change of damage and C_{ijkl} are the compliance tensor components.

The model does not present a relation between the compliance tensor $\mathbf{C}$ and the damage variable D but just the relation between the stiffness tensor $\mathbf{E}$ and the damage. The tensor $\bar{\mathbf{M}}$ is presented in equation (38), in which the stiffness tensor is defined in terms of the damage variable:

$$\bar{M}_{ijkl} = \frac{\partial E_{ijkl}}{\partial \bar{D}}\bar{\mathscr{M}}. \tag{38}$$

The direction of the rate of change of the damage in the stiffness space, $\bar{\mathscr{M}}$, is given by:

$$\bar{\mathscr{M}} = \frac{\partial Q}{\partial(-\bar{Y})} = \frac{\partial Q}{\partial(-Y)}, \tag{39}$$

where $-\bar{Y} = -Y$, according to equation (40):

$$\bar{Y} \equiv \frac{\partial \psi^d}{\partial D} = -\frac{1}{2}\varepsilon^e_{kl}E^0_{klij}\varepsilon^e_{ij} = Y = -\frac{1}{2(1-D)^2}\sigma_{kl}C^0_{klij}\sigma_{ij}. \tag{40}$$

Thus, $\bar{\mathscr{M}}$ is define by:

$$\bar{\mathscr{M}} = \frac{1}{(1-D)}\left(\frac{-\bar{Y}}{r}\right)^S. \tag{41}$$

E_{ijkl} is written as:

$$E_{ijkl} = (1 - D)E^0_{ijkl}, \tag{42}$$

whose derivative of equation (38) is:

$$\frac{\partial E_{ijkl}}{\partial D} = -E^0_{ijkl}. \tag{43}$$

Substituting equations (39) and (43) in equation (38), it is obtained $\bar{M}_{ijkl}$ as:

$$\bar{M}_{ijkl} = -(E^0_{ijkl})\frac{1}{1-D}\left(\frac{-\bar{Y}}{r}\right)^S. \tag{44}$$

As in equation (**??**) it is necessary to determine $\mathbf{M}$, it is possible to relate M_{ijkl} with $\bar{M}_{ijkl}$ by the following expression:

$$M_{ijkl} = -C_{ijpq}\bar{M}_{pqrs}C_{rskl}. \tag{45}$$

Performing calculations, M_{ijkl} is defined by:

$$M_{ijkl} = C_{ijkl}\frac{1}{1-D}\left(\frac{-Y}{r}\right)^S. \tag{46}$$

Substituting equation (46) in equation (**??**), m_{ij} is defined as:

$$m_{ij} = \frac{1}{1-D}\left(\frac{-Y}{r}\right)^S C_{ijkl}\sigma_{kl}. \tag{47}$$

The equations (48), (49) and (50) present the relation between $\bar{\mathbf{n}}$ and $\mathbf{n}$, $\bar{\mathbf{m}}$ and $\mathbf{m}$ and $\bar{\mathbf{H}}$ and $\mathbf{H}$, respectively, according to Penna (2011):

$$\bar{n}_{ij} = E_{ijkl}n_{kl}\ , \tag{48}$$

$$\bar{m}_{ij} = -E_{ijkl}m_{kl}\ , \tag{49}$$

$$\bar{H} = H + n_{ij}E_{ijkl}m_{kl}\ , \tag{50}$$

where $\mathbf{n}$, $\mathbf{m}$ and $\mathbf{H}$ are formulated in the stress space and $\bar{\mathbf{n}}$, $\bar{\mathbf{m}}$ and $\bar{\mathbf{H}}$ in the strain space.

From these relations, in both models based on stress and strain may be inserted on the theoretical and computational environment to constitutive models.

Therefore, in the strain space, $\bar{n}_{kl}$, $\bar{m}_{kl}$ and $\bar{H}$ are written as:

$$\bar{n}_{kl} = E_{ijkl}\sqrt{\frac{3}{2}}\frac{s_{kl}}{(1-D)\|s_{kl}\|}\ , \tag{51}$$

$$\bar{m}_{ij} = -E_{ijkl}\frac{1}{1-D}\left(\frac{-\bar{Y}}{r}\right)^S\varepsilon_{kl}\ , \tag{52}$$

and

$$\bar{H} = \mathscr{H} + n_{ij} E_{ijkl} m_{kl} \ . \tag{53}$$

The substitution of equations (51), (52) and (53) in equation (31) leads to an expression to the tangente operator:

$$E^t_{ijkl} = E_{ijkl} + \frac{1}{\mathscr{H} + n_{ij} E_{ijkl} m_{kl}} (-E_{ijkl}) \frac{1}{1-D} \left(-\frac{\bar{Y}}{r} \right)^S \varepsilon_{kl} E_{ijkl} \sqrt{\frac{3}{2}} \frac{s_{kl}}{(1-D)\|s_{kl}\|} \ . \tag{54}$$

4 FORMULATION OF THE GFEM

The Generalized Finite Element Method (GFEM) can be considered a variation of the conventional Finite Element Method (FEM). According to Barros (2002), GFEM was independently proposed by:
– Babuška and colleagues under the names Special Finite Element Method (Babuška and Caloz, 1994) and posteriorly Partition of Unity Method;
– Duarte and J. T. Oden under the name *hp* clouds, hybrid formulation of the FEM (Duarte and Oden, 1995 and Duarte and Oden, 1996a).

Barros (2002) also highlighted that the current denomination of GFEM was first used by Melenk and Babuška (1996). According to Duarte *et al.* (2000), several of the so-called meshless methods proposed can also be viewed as special cases of the GFEM. This is due to the fact that these methods use a Partition Unity (PU), which is a set of functions whose values sum to the unity at each point x in a domain Ω guaranteing element continuity. Alves *et al.* (2013) affirmed that such strategy creates conforming approximations which are improved by a nodal enrichment scheme.

The paper of Duarte and Oden (1996b) presents a meshless method so-called *hp*-Cloud Method in which clouds (sets) of points are used to discretize the problem domain and form the basis to build the approximation. The approximation functions of GFEM are build in a similar way, but, differently, it is the patch of elements that defines the cloud over which the Lagrangian Finite PU is defined. The use of functions of PU, on a finite element mesh, and the enrichment of these functions by the same scheme of the *hp*-Cloud Method allow the interpretation of GFEM as a nonconventional form of FEM, establishing a relation with meshless methods.

The strategy used in GFEM consists of employing functions of the type PU that enriched define the shape functions. The conventional functions of FEM (such as Lagrangian functions) facilitates the application of the GFEM and, differently from the meshless methods, directly verifies the boundary conditions (Barros (2002)).

The clouds are formed by sets of finite elements that share the same nodal points x_j (on Fig. 1 represented by ω_j). For example, in $\mathbb{R}^1$ the PU is formed with the use of linear Lagrangian functions (on Fig. 1 represented by $\mathcal{N}_j(x)$).

The Lagrangian Finite Element functions N_j, associated with each one of the n nodes, can be considered as a PU because for any position x:

$$\sum_{j=1}^{n} \mathcal{N}_j(x) = 1. \tag{55}$$

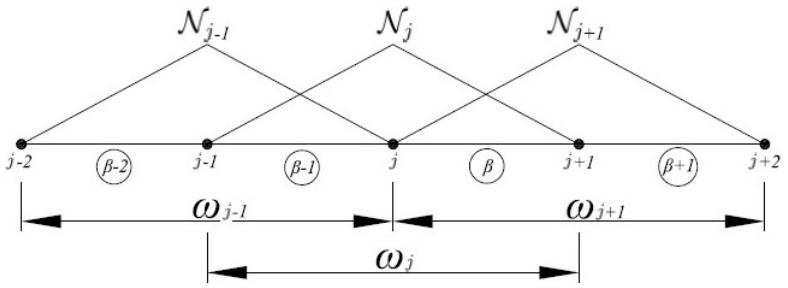

Figure 1: Partition of Unity from finite elements in $\mathbb{R}^1$ (Alves (2012)).

The enrichment functions, typically used in *hp*-Cloud Method, are multiplied by the original PU, guaranteeing the improvement of the quality of the approximation. Aiming to clarify these strategy, it is considered a conventional mesh of finite element defined from a set of n nodal points $\{x_j\}_{j=1}^n$, according to Fig. 2(a), in $\mathbb{R}^2$. It is defined a patch or cloud ω_j formed by all elements that share the nodal point x_j.

The set of interpolative Lagrangian functions associated with the node x_j defines the function $\mathcal{N}_j(x)$ whose support corresponds to the region ω_j, according to Fig. 2(b).

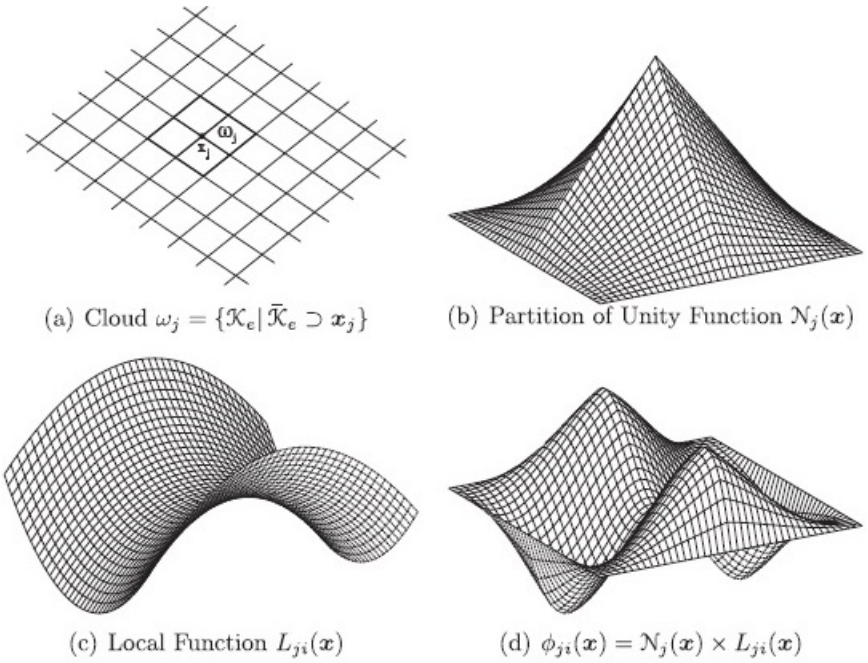

Figure 2: Strategy of enrichment of the cloud ω_j (Barros (2002)).

A set of enrichment functions, so-called local approximation functions, is composed by q_j linearly independent functions defined to each node x_j with support on the cloud ω_j:

$$\mathcal{I}_j = \{L_{j1}(x), L_{j2}(x), ..., L_{jq}(x)\} = \{L_{ji}(x)\}_{i=1}^q, \;\; with \; L_{ji}(x) = 1. \tag{56}$$

At the end of the process, the shape functions $\phi_{ji}(x)$ of GFEM, shown on Fig. 2(d), associated with the node x_j are built through the enrichment of the PU functions by the components of the set $\mathcal{I}_j$. Thus, according to the Eq. (57), $\phi_{ji}(x)$ can be obtained by the product between

the basic functions that form the PU (Fig. 2(b)) and the enrichment functions (Fig. 2(c)).

$$\{\phi_{ji}\}_{i=1}^{q} = \mathcal{N}_j(x) \times \{L_{ji}\}_{i=1}^{q} \ \ (no\ summation\ on\ j). \tag{57}$$

The functions of the Eq. (56) can be polynomial or not depending on the problem analyzed. The use of the functions of FEM as the PU simplifies the implementation and avoids, according to Barros (2002), problems related to the numerical integration and to the imposition of the boundary conditions.

Thus, a generic approximation $\tilde{u}$ is obtained by the following linear combination of the shape functions:

$$\tilde{u}(x) = \sum_{j=1}^{N} \mathcal{N}_j(x) \left\{ u_j + \sum_{i=2}^{q} L_{ji}(x) b_{ji} \right\}, \tag{58}$$

where u_j and b_{ji} are nodal parameters associated with standard ($\mathcal{N}_j$) and GFEM ($\mathcal{N}_j \times L_{ji}(x)$) shape functions, respectively.

Furthermore, aiming to minimize round-off errors, Duarte *et al.* (2000) suggested that a transformation should be performed over the $L_{ji}(x)$ functions, when they are of polynomial type. In such case, the coordinate x is replaced as follows:

$$x \rightarrow \frac{x - x_j}{h_j}, \tag{59}$$

in which h_j is the diameter of the largest finite element sharing the node j.

It is obtained the product function that presents the approximative characteristics of the local approximation function while inherits the compact support of the PU.

The approximation functions, with monomials expressed in coordinate x, used to the analysis are defined by:

- $P0$ (No Enrichment):

$$\phi_j^T(x) = [\mathcal{N}_j(x)]; \tag{60}$$

- $P1$ (Linear Enrichment):

$$\phi_j^T(x) = \left[\mathcal{N}_j(x) \quad \mathcal{N}_j(x) \left(\frac{x - x_j}{h_j} \right) \right]; \tag{61}$$

- $P2$ (Quadratic Enrichment):

$$\phi_j^T(x) = \left[\mathcal{N}_j(x) \quad \mathcal{N}_j(x) \left(\frac{x - x_j}{h_j} \right) \quad \mathcal{N}_j(x) \left(\frac{x - x_j}{h_j} \right)^2 \right]. \tag{62}$$

The approximation functions, with monomials expressed in coordinates x and y, used to the analysis are defined by:

- $P0$ (No Enrichment):

$$\phi_j^T(x) = \begin{bmatrix} \mathcal{N}_j(x) & 0 \\ 0 & \mathcal{N}_j(x) \end{bmatrix}; \tag{63}$$

- $P1$ (Linear Enrichment):

$$\phi_j^T(x) = \begin{bmatrix} \mathcal{N}_j(x) & 0 & \mathcal{N}_j(x)\left(\frac{x-x_j}{h_j}\right) & 0 & \mathcal{N}_j(x)\left(\frac{y-y_j}{h_j}\right) & 0 \\ 0 & \mathcal{N}_j(x) & 0 & \mathcal{N}_j(x)\left(\frac{x-x_j}{h_j}\right) & 0 & \mathcal{N}_j(x)\left(\frac{y-y_j}{h_j}\right) \end{bmatrix}; \quad (64)$$

- $P2$ (Quadratic Enrichment):

$$\phi_j^T(x) = \mathcal{N}_j(x) \begin{bmatrix} 1 & 0 & \left(\frac{x-x_j}{h_j}\right) & 0 & \left(\frac{y-y_j}{h_j}\right) & 0 & \left(\frac{x-x_j}{h_j}\right)^2 & 0 & \left(\frac{y-y_j}{h_j}\right)^2 & 0 \\ 0 & 1 & 0 & \left(\frac{x-x_j}{h_j}\right) & 0 & \left(\frac{y-y_j}{h_j}\right) & 0 & \left(\frac{x-x_j}{h_j}\right)^2 & 0 & \left(\frac{y-y_j}{h_j}\right)^2 \end{bmatrix}. \quad (65)$$

5 NUMERICAL EXAMPLE

According to Mashayekhi *et al.* (2005), tensile tests are performed in both numerical and experimental analyzes aiming to investigate brittle fracture. This test is carried out here to demonstrate the versatility of GFEM nonlinear implementation combined with elastoplastic damage constitutive model of Lemaitre (1985a,1985b).

The specimen, shown at Figure 3, has been evaluated to a two-dimensional discrete model. The results presented by Mashayekhi *et al.* (2005) refer to the three-dimensional model. This element under tensile experiences a characteristic *stress-strain* behavior that induces crack initiation at the center and its propagation toward the outer edge.

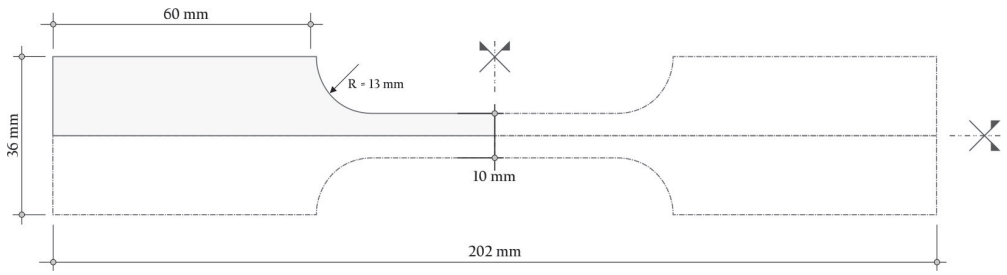

Figure 3: Dimensions of the specimen.

The finite element mesh, with 125 elements, discretizes a quarter of the element geometry and appropriate boundary are imposed at the edges, as presented at Fig. 4.

To the numerical simulations, it was adopted plan stress conditions, $5\ mm$ of thickness and generalized displacement control method, with load factor of $0,10$, tolerance of 1×10^{-4} and reference load of $-860\ N/mm$. Two simulations have been performed aiming to validate the GFEM implementation, comparing the results to GFEM enriched and to GFEM without enrichment (reproducing FEM):

- $GFEM - Q4 - P1$: quadrilateral finite elements with four nodes and all nodes are enriched with the linear function $P1$ (in coordinates x and y), resulting in a quadratic shape function;
- $GFEM - Q8 - P0$: quadrilateral finite elements with eight nodes and no nodes are enriched, with quadratic shape functions reproducing FEM.

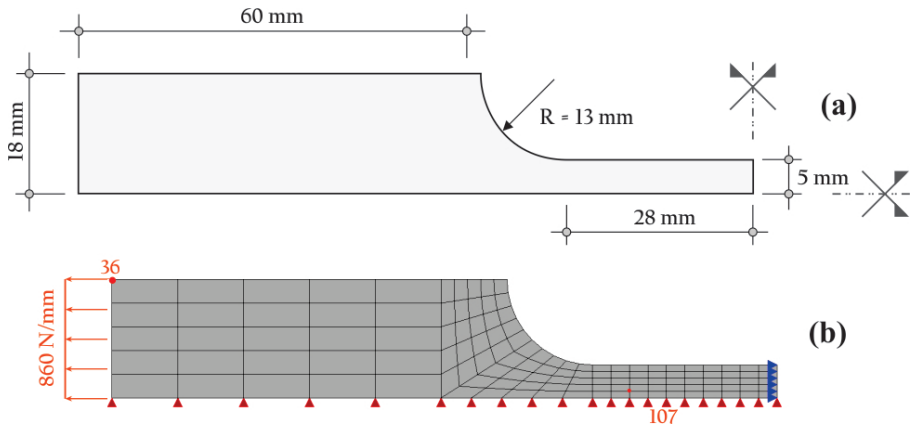

Figure 4: Direct tensile test: (a) a quarter of geometry; (b) finite element mesh.

The material used is the steel AISI 1010 whose parameters are: $E = 210000\ MPa$, $\nu = 0.30$, $\sigma_0 = 620\ MPa$, $r = 3.50\ MPa$ (damage resistence) and $S = 1$ (damage exponent); Benallal *et al.* (1987) calibrated a function $\sigma(\kappa)$ to this material, whose parameters are: $a = 3300$, $b = 0.40$, $H(\kappa) = a \cdot b\, e^{-0.40\kappa}$, where H is the hardening or softening function and κ is a hardening or softening variable.

Mashayekhi *et al.* (2005) defined a limit load to the yield stress as $P_L = -15500\ N$. Thus, it is possible obtain a normalized by the relation P/P_L. The responses *normalized load* P/P_L x *horizontal displacement* at the node 36 (indicated in the Fig. 4 (b)) to the simulations $GFEM - Q4 - P1$ (graphic (a)) and $GFEM - Q8 - P0$ (graphic (b)) are illustrated at Fig. 5, together with the numerical results obtained by Mashayekhi *et al.* (2005) (graphic (c)).

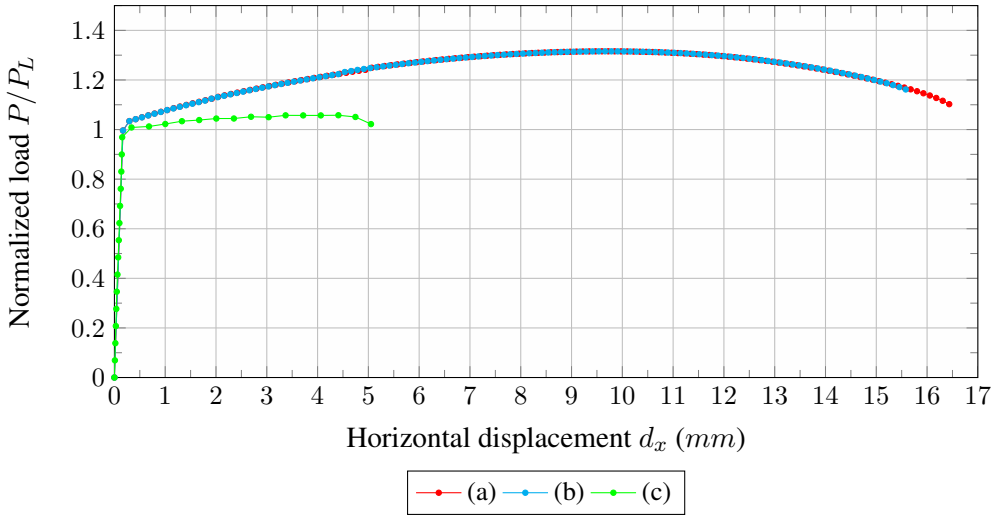

Figure 5: ***Normalized load*** **(**P/P_L**) x** ***horizontal displacement*** **(**d_x**) : (a)** $GFEM - Q4 - P1$**; (b)** $GFEM - Q8 - P0$**; (c) Mashayekhi *et al.* (2005) model.**

It is verified in the graphics (a) and (b) the influence of damage process on the global behavior of the structure. With the occurrence of softening, the load capacity of the specimen decreased. Comparing the numerical result presented by Mashayekhi *et al.* (2005) with the ones obtained with the application of the Lemaitre (1985a,1985b) model, it is verified that the behavior are similar. The differences between the responses can be explained by the fact that it was applied different types of elements, integration algorithms and analysis model. The simulations $GFEM - Q8 - P0$ and $GFEM - Q4 - P1$ shown the same responses, but the last one achieved a larger displacement.

From the results shown in the graphics (a) and (b), it is possible verify in the Fig. 6 the damage evolution and the behavior of stress σ_{xx} in relation to strain ε_{xx}, to the node 107 (the region of this node presented the most intense degradation). There were the growth of damage and stress values and the decline of the latter during the loading process caused by damage influence for both simulations. The responses of the simulation $GFEM - Q4 - P1$ captured a larger stress degradation and growth of the damage than the simulation $GFEM - Q8 - P0$. To this, the maximum damage value is $D = 0.8631$ while to the simulation $GFEM - Q4 - P1$ damage is $D = 0.9029$.

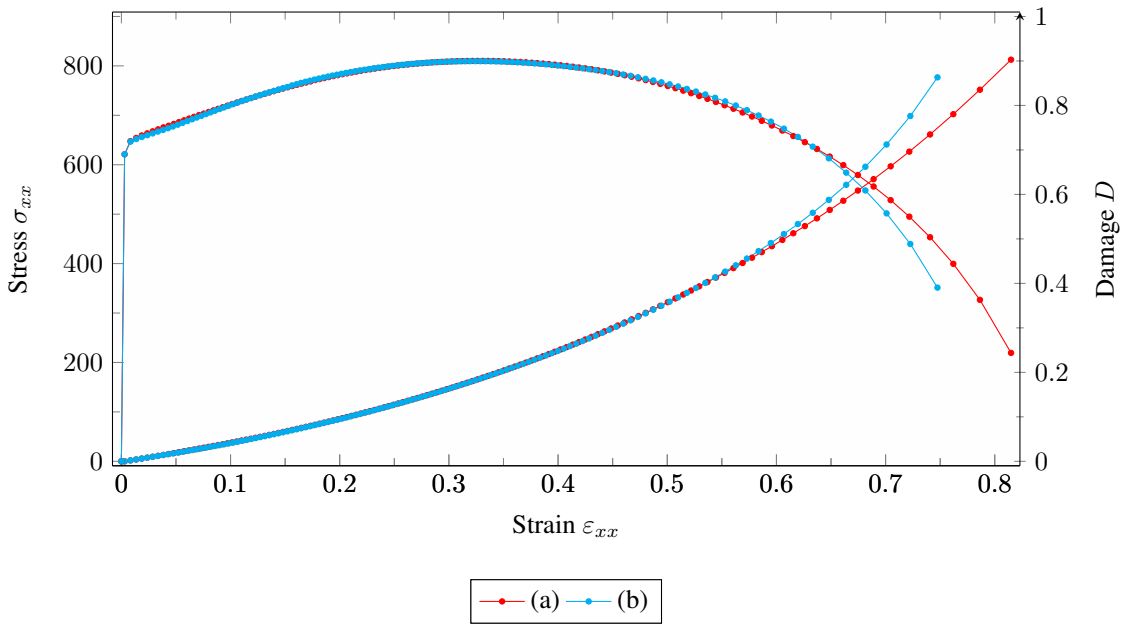

Figure 6: ***Stress*** **(**σ_{xx}**) x** ***strain*** **(**ε_{xx}**) and** ***damage*** **(**D**) x** ***strain*** **(**ε_{xx}**) at node** 107**: (a)** $GFEM - Q4 - P1$**; (b)** $GFEM - Q8 - P0$

Regarding the damage distribution along analyses, Fig. 7 and 8 present its evolution respectively to $GFEM - Q4 - P1$ and $GFEM - Q8 - P0$. At the beginning of the loading for both simulations, damage presented low values and it was concentrated at the central region of the specimen.

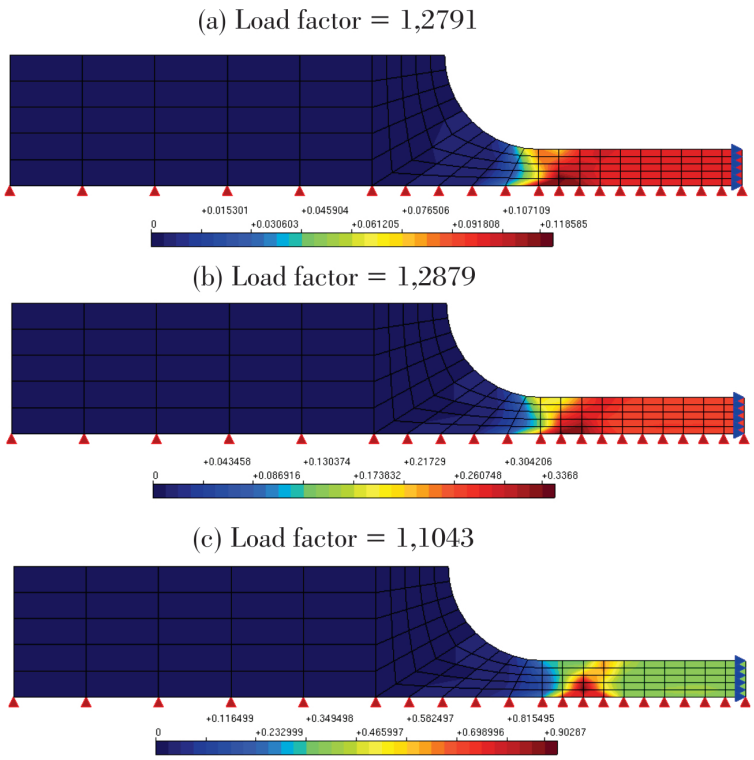

Figure 7: $GFEM - Q4 - P1$

The maximum damage achieved in the simulation $GFEM - Q4 - P1$ was $D = 0.9029$ (Fig. 7 (c)) around the region of the node 107. To the simulation $GFEM - Q8 - P0$, the maximum damage was $D = 0.8631$ (Fig. 8 (c)) concentrated at the node 107.

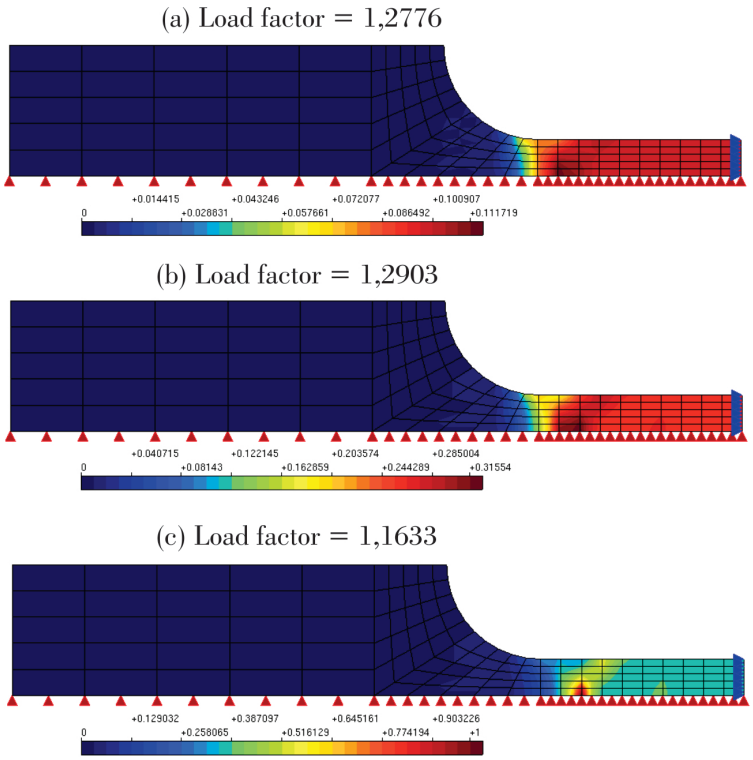

Figure 8: $GFEM - Q8 - P0$

In this sense, Mashayekhi *et al.* (2005) shown that to some notched specimens subjected to direct tensile test, the damage process is initiated at is center and propagates in direction to the edges of the element.

6 CONCLUSIONS

This paper has presented a general idea about the Elastoplastic Damage Constitutive Model proposed by Lemaitre (1985a,1985b), its implementation on the Unified Theoretical and Computational Environment (Penna 2011) and the formulation of GFEM.

The computational efficiency, application with together elastoplastic damage constitutive model of Lemaitre (1985a,1985b) and validation of the GFEM framework to nonlinear analysis is demonstrated by numerical example. In a general view, the obtained results can qualitatively show that the GFEM framework to nonlinear analysis is able to produce good results. New investigations must be performed aiming to verify the numerical stability of GFEM applied to the nonlinear analysis, mainly when its application requires enrichments of higher orders or a large numberof finite elements.

ACKNOWLEDGEMENTS

The authors gratefully acknowledge the important support of the Brazilian research agencies CNPq (in Portuguese ”Conselho Nacional de Desenvolvimento Científico e Tecnológico”

- Grants 309005/2013-2, 486959/2013-9, and 308785/2014-2) and FAPEMIG (in Portuguese "Fundação de Amparo à Pesquisa de Minas Gerais" - Grant PPM-00669-15).

REFERENCES

Alves, P. D., 2012. *Estratégia global-local aplicada ao Método dos Elementos Finitos Generalizados*. MSc. thesis, Universidade Federal de Minas Gerais, Brazil.

Alves, P. D., Barros, F.B., Pitangueira, R. L. S., 2013. An object-oriented approach to the generalized finite element method. *Advances in Engineering Software*, vol. 59, pp. 1-18.

Babuška I. and Caloz, G. O. J. E., 1994. Special finite element method for a class of second order elliptic problems with rough coefficients. *SIAM Journal on Numerical Analysis*, vol. 36, pp. 3553-3576.

Barros, F.B., 2002. *Métodos sem malha e método dos elementos finitos generalizados em análise não linear de estruturas*. Ph.D. thesis, Universidade de São Paulo, São Carlos, SP, Brazil.

Benallal, A., Billardon, R., Doghri, I. and Moret-Bailly, L., 1987. Crack initiation and propagation analyses taking into account initial strain hardening and damage fields. *Fourth Int. Conf. of Numerical Methods in Fracture Mechanics*, Texas, EUA.

Carol, I., Rizzi, E., Willam, K. 1994. A unified theory of elastic degradation and damage based on a loading surface. *International Journal of Solids Structures*, vol. 31, pp. 2835-2865.

Coleman, B. D. and Gurtin, M. E., 1967. Thermodynamics with internal state variables. *Journal of Chemistry and Physics*, vol. 47, pp. 597-613.

Duarte, C. A. M. and Oden, J. T., 1995. Hp-clouds - a meshless method to solve boundary value problem. *Technical Report*, TICAM, The University of Texas at Austin.

Duarte, C. A. M. and Oden, J. T., 1996a. An hp-adaptive method using clouds. *Computer Methods in Applied Mechanics and Engineering*, vol. 139, pp. 237-262.

Duarte, C. A. M. and Oden, J. T., 1996b. Hp-clouds and hp-meshless method. *Numerical Methods for Partial Differential Equations*, vol. 12, pp. 673-705.

Duarte, C. A., Babuška, I., Oden, J. T., 2000. Generalized finite element methods for three-dimensional structural mechanics problems. *Computers and Structures*, vol. 77, pp. 215-232.

Lemaitre, J., 1985a. A continuous damage mechanics model for ductile fracture. *Journal of*

Engineering Materials Technology, vol. 107, pp. 83-89.

Lemaitre, J., 1985b. Coupled elasto-plasticity and damage constitutive equations. *Comp. Meth. Appl. Mech. Engng*, vol. 51, pp. 31-49.

Lemaitre, J. and Chaboche, J. L., 1990. *Mechanics of solid materials*. Cambridge University Press.

Lemaitre, J., Sermage, J. P. and Desmorat, R., 1999. A two scale damage concept applied to fatigue. *Tech Science Press*, vol. 97, pp. 67-81.

Mashayekhi, M., Ziaei-Rad, S., Parvizian, J., Nikbin, K. and Hadavinia, H., 2005. Numerical analysis of damage evolution in ductile solids. *Tech Science Press*, vol. 1, pp. 65-82.

Melenk, J. M. and Babuška, I., 1996. The partition of unity finite element method: basic theory and applications. *Computer Methods in Applied Mechanics and Engineering*, vol. 139, pp. 289-314.

Monteiro, A. B., 2013. *Ambiente Teórico-Computacional Unificado para Modelos Constitutivos: Inclusão de Modelo Elastoplástico com Dano*. Master's thesis, Universidade Federal de Minas Gerais, Brazil.

Murakami, S., 2012. *Continuum Damage Mechanics*. Springer, Nagoya, Japão.

Penna, S. S., 2011. *Formulação multipotencial para modelos de degradação elástica: Unificação teórica, proposta de novo modelo, implementação computacional e modelagem de estruturas de concreto*. Ph.D. thesis, Universidade Federal de Minas Gerais, Brazil.